2017

Toll-like receptor 7: Expression patterns within mammalian Trigeminal and Dorsal Root Ganglia and its selected facial innervation target, the tongue

Kawamura, S.

Kawamura, S. (2017) ' Toll-like receptor 7: Expression patterns within mammalian Trigeminal and Dorsal Root Ganglia and its selected facial innervation target, the tongue', The Plymouth Student Scientist, 10(2), p. 59-79.
http://hdl.handle.net/10026.1/14161

The Plymouth Student Scientist
University of Plymouth

Toll-like receptor 7: Expression patterns within mammalian Trigeminal and Dorsal Root Ganglia and its selected facial innervation target, the Tongue.

Sara Kawamura

Project Advisor: Stephen W. N. Thompson, School of Biomedical and Healthcare Sciences, Plymouth University Peninsula Schools of Medicine and Dentistry, Plymouth University, Drake Circus, Plymouth, Devon PL4 8AA, UK

Abstract

Toll-like receptors (TLRs) are known to be expressed in the mammalian nervous system where they play an important role in the hosts' immune defence against bacterial and viral pathogens. Recent studies have looked into the expression of a wide range of TLRs in various neuronal sub-populations of the central and peripheral nervous systems. However, the co-expression of TLRs within the sub-populations of neurons as well as the expression of TLRs in the terminals of various innervation targets are yet to be understood. In this study, Immunohistochemistry was used to quantify the expression of TLR7 with known neurochemical markers in two sets of tissue samples from the cephalic nervous system of naïve rats, namely, the Trigeminal Ganglia (TG) and one of its innervation targets, the Tongue. The patterns of TLR7 expression within the TG were compared to that of the Dorsal Root Ganglia (DRG) of the same naïve rat, which showed no significant difference. Although very little co-localization was seen between TLR7 and its co-stained neurochemical markers, NF200 and IB4, more co-localization was seen with IB4 than with NF200. On the other hand, the peripheral nerves innervating the tongue showed unique structures that allowed the identification of the origin of the nerve bundles, in addition to revealing the identity of each axon within each nerve bundle. These results indicate that TLR7 may play a distinct role in the response to pathogens within the tongue, which provides a basis for further studies on the specificity of TLR7 in the peripheral nerves.

Introduction

Toll-like receptors (TLRs) are transmembrane proteins that belong to the family of pattern recognition receptors (PRRs) (Kumar, Kawai and Akira, 2009). They are expressed on the cells of the innate immune system (Iwasaki and Medzhitov, 2010), and are well understood for their involvement in the detection of various infectious microorganisms (Takeda, Kaisho and Akira, 2003; Wei et al., 2017). TLRs are capable of mediating immune responses through the recognition of exogenous pathogen associated molecular patterns (PAMPS) (Iwasaki and Medzhitov, 2004; Roach et al., 2005), and endogenous danger associated molecular patterns (DAMPS) (Imai et al., 2008; Midwood et al., 2009; West et al., 2010). The involvement of TLRs in the innate immunity was first described in the toll family of proteins in drosophila (Hashimoto, Hudson and Anderson, 1988). Hitherto, a total of thirteen functional TLRs (TLR1-TLR13) have been identified in humans and mice, where they were found to be constitutively expressed in both the central (CNS) and peripheral (PNS) nervous systems (Wei et al., 2017; Lafon et al., 2006; Mishra, Mishra and Teale, 2006; Bsibsi et al., 2002; Wadachi and Hargreaves, 2006; Cameron et al., 2007; Barajon et al., 2009). The gene of TLR7 is located on the proximal region of the chromosomal locus Xp22, and is encoded by three exons (Du et al., 2000). Studies have shown that TLR7 is expressed strictly in small diameter unmyelinated c-fibre peptidergic nociceptive sensory neurones that are neurofilament-negative (Liu et al., 2010; Qi et al., 2011; Barajon et al., 2009; Park et al., 2014; Helley et al., 2015). However, it is also expressed occasionally in small diameter unmyelinated c-fibre non-peptidergic, or medium diameter thinly myelinated Aδ sensitive neurones (Bennet et al., 1998).

TLR7 belongs to the nucleic acid-sensing subgroup that allows it to respond to viral single-stranded RNA (ssRNA) (Wei et al., 2017), in addition to small purine analogue compounds such as imidazoquinolines that are frequently used in antiviral treatments. Furthermore, TLR7 mediates nociception through the ion channels of heat-sensitive TRPV1 and cold-sensitive TRPA1 during tissue injury (Basbaum et al., 2009; Woolf and Ma, 2007; Liu et al., 2010; Qi et al., 2011; Park et al., 2014). Activation of TLR7 initiates immune responses via transcriptional regulation by activating the MyD88-dependent pathway leading to the production of type I IFNs and inflammatory cytokines. TLR7 are located mostly on the membranes of the endoplasmic reticulum (ER) and are recruited to the endosomes following the stimulation of their ligands, although this mechanism still needs to be clarified (Takeuchi and Akira, 2010).

TLR7 immunoreactivity is present in the terminals of the sensory neurons of the spinal cord (Liu et al., 2010). A study conducted by Mishra, Mishra and Teale (2006) shows the role of TLR7 in the interplay of immune cells and CNS cells during infection, and was thought to be a part of the innate immune response that mediated neuroprotection. Meanwhile, a study conducted by Liu et al. (2010) shows that TLR7 is expressed in nerve branches of the dermis and the nerve terminals of the epidermis of the skin. Thus, it is likely that TLR7 is transported from the sensory neuron cell bodies in the TG and DRG, to the nerves of the skin, and may possibly be expressed in other peripheral nerve terminals to aid in the mediation of pruritus (Liu et al., 2010). TLR7 is expressed by 30% of small diameter nociceptive primary sensory neurons in the DRG (Schmelz et al., 1996; Liu et al., 2010; Park et al., 2014). Meanwhile, other studies show that TLR7 is expressed in around 32.4%+-1.8 within the total cell profile in the TG (Helley et al., 2015) and 35%+- 3.9% to 46.7% +-1.9% of the total cell profile within the DRG (Bennet et al., 1998; Park et al., 2014).

The TG and DRG contain the cell bodies of various subpopulations of nociceptors, which are a specialized class of primary sensory neurons that respond to stimulus intensity of noxious range, suggesting that they possess biophysical and molecular properties. These biophysical and molecular properties enable them to selectively detect and respond to potentially damaging stimuli. The stimuli are detected by the cell bodies which give rise to a single axon that bifurcates into two branches; the first being the peripheral branch which innervates peripheral target tissues; the second being the central axon that enters the CNS to synapse on second order nociceptive neurons (Woolf and Ma, 2007; Basbaum et al., 2009). Nociceptors have four major functional components: the cell body that is responsible for controlling the integrity and the identity of the neuron, the axons that are responsible for the conduction of action potentials, the peripheral terminal which transduces external stimuli and initiates the action potential, and the central terminal that forms a presynaptic element of the first synapse on the sensory pathway in the CNS. In addition to the intrinsic properties of the neuron to its functional role, the extrinsic signals are as crucial, feeding the neuron with signals from targets, nerves, and the spinal cord that produce profound phenotypic alterations (Woolf and Ma, 2007).

While studies show that TLR7 is only expressed in discrete sub-populations of the neuronal cells in the DRG, only a few studies have looked into its expression within the TG. This study aims to determine the exact sub-populations in which TLR7 is expressed in the TG by using an antibody technology to compare both qualitative and quantitative data against that of the DRG. Two well-defined neurochemical markers were used to determine low threshold Neurofilament 200 (NF200) expressing myelinated A-fibre nociceptive neurones, and high threshold Isolectin-B4 (IB4) expressing unmyelinated c-fibre non-peptidergic neurones. A process of elimination was used to reveal TLR7 expressing high threshold c-fibre peptidergic nociceptive neurones. In addition, a process of elimination was used to reveal co-expression of TLR7 with NF200 and IB4 expressing subpopulations. Moreover, the TG and DRG form a passage area in which axons are passing through the ganglion and innervating various peripheral target tissues. Although TLR7 expression had been looked into in the skin of mammals, the trigeminal system has not been investigated. This study aims at following the axons of the neurones from the TG into one of its peripheral innervation targets, the tongue, to try and determine the expression, distribution and co-localisation of TLR7 with its selected neurochemical markers.

Materials and methods

Tissue preparation

Three naïve adult male rats (150-200g) were euthanised with adhesion to the prescribed guidelines of Schedule 1 of the UK 1986 Animals (Scientific Procedures) Act. Animals were transcardially perfused with 0.1M of phosphate buffer saline (PBS, pH 7.4) followed by 4% paraformaldehyde in 0.1M phosphate buffer (pH 7.4). The DRG, TG and tongue tissues were dissected and placed in a post-fix solution of 4% paraformaldehyde (pH 7.4) for 2 hours at 4°C. Subsequently, specimens were transferred to an overnight cryoprotectant solution of 20% sucrose in 0.1M phosphate buffer (pH 7.4) at 4 °C. Tissue samples were snap-frozen in an optimal cutting temperature compound (Tissue Tek, UK) on dry ice at -80°C. The tissue sections were transversely cryosectioned to 10 micrometres (CM1100, Leica Biosystems, Milton-

Keynes, UK). Three slides were prepared for each tissue and eight tissue sections of the same tissue were placed on each slide. All slides were incubated in 30% cryoprotectant solution and stored over night at -20 °C.

Immunohistochemistry

All tissue sections were washed in PBS and blocked with donkey serum (10% PBS, 0.2% Trixon-x-100, 0.1% azide) and placed in a covered humidity chamber at room temperature for 1 hour. Sections underwent further PBS washes before the primary antibodies of rabbit anti-TLR7 (1:500 Novus Biologicas, Littleton, CO, USA) and mouse anti-NF200 (1:4000, Sigma-Aldrich, Gillingham, UK) were pooled onto the slides. All slides were subsequently incubated for 24 hours at room temperature with the exception of tongue tissues, which used a combination of rabbit anti-TLR7 and Isolectin-B4 Fluorescein isothiocyanate (IB4-FITC) (10µg/m, Sigma-Aldrich, Gillingham, UK) primary antibodies, and were incubated in the dark. Following PBS washes, the tissue sections were incubated with a combination of secondary antibodies of donkey anti-rabbit alexa fluor (AF) -555 (10µg/ml, Abcam, Cambridge, UK) and donkey anti-mouse FITC (1:200, Abcam, Cambridge, UK), with the exception of the tongue which was incubated with donkey anti rabbit AF-555 only. Sections were left in the dark at room temperature for 3 hours. Slides were subsequently washed with PBS and incubated with 4'6-diamidino-2-phenylinodile (DAPI) (100ng/mL, Sigma-Aldrich, Gillingham, UK) for 1 hour in a covered humidity chamber at room temperature. Tissue sections were washed with PBS for the final time and mounted in FluorSave (EMD Millipore, Watford, UK).

Imaging and analysis

Each tissue section on the prepared slides were divided into three fields and captured at x100 and x200 magnifications under an epifluorescence microscope (Nikon eclipse 80i) equipped with a Nikon DSQi1Mc camera, and using NIS-elements software (BR 3.2, Nikon, New York, NY, USA). The same NIS-elements software was used to count neuronal body profiles from TG and the DRG, while tongue sections were analysed qualitatively. A TG and DRG image quantification was performed on a monochrome image by a single investigator; only neuronal profiles with visible nuclear DAPI counterstains were included in the counting process. Subjective visual criteria were used to determine positive TLR7 immunoreactivity (IR). A mean fluorescence intensity unit was used to set the threshold for positive counting for each antibody. Following identification of positive profiles in individual images, co-expression of TLR7 with its phenotypic markers were observed in the overlaid images. The mean number of TLR7 expressing cells, NF200 expressing cells and co-expressing cells were determined. Mean numbers were used to calculate the significance of TLR7 expressing cells within the total number of neuronal cells across TG and DRG, using an independent T-test (IBM SPSS 23 software). Co-expression was demonstrated as a percentage of target markers exhibiting the phenotypic markers and vice-versa which were plotted as a stacked bar chart (windows excel 2013).

Results

Expression of TLR7 within the adult mammalian TG and DRG

TLR7 expression was determined by indirect single-labelling immunohistochemistry within the TG and DRG of three naïve male adult rats. Multiple neuronal profiles displayed TLR7 immunoreactivity in the TG and DRG (Fig. 1).

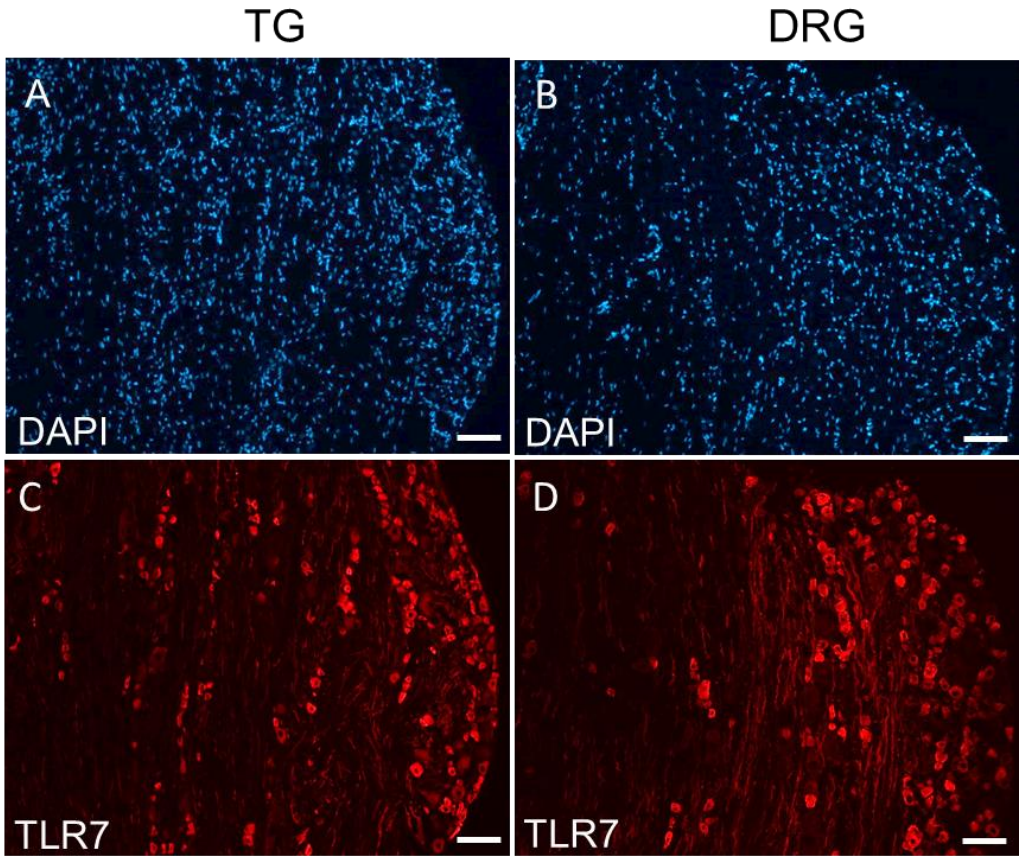

Fig. 1. Expression of TLR7 within the TG and DRG. Visible neuronal (large faint blue) nuclear and non-neuronal (small bright blue) DAPI counterstains within the TG (A) and DRG (B). Multiple neuronal profiles and its axons displaying intracellular granular IR for TLR7 (red) within the TG (C) and DRG (D), although not all neuronal cell bodies and axons displayed TLR7-IR. All non-neuronal cells within the tissues are shown to be negative for TLR7. Scale bar 100µm.

Three types of cell nuclei were observed within the TG and DRG that were stained with DAPI (Fig.1A and B). The neuronal cell nuclei were distinguished from non-neuronal cell nuclei by the size of the nucleus and the density in which DAPI had been taken up. Neuronal cell nuclei were observed as large round profiles that were very faint in colour, and were scattered across the tissue section. Conversely, non-neuronal nuclei were much smaller in size, and took up a large density of the DAPI stain, giving off a bright blue fluorescent colour and was much more abundant throughout the tissue sections. Among the brightly stained non-neuronal cell nuclei, two types of nuclei were observed; the first type belonging to Satellite glial cells with round profiled nuclei, and the second type belonging to Schwann cells with longer profiled nuclei. The nuclei of the satellite cells and Schwann cells were arranged in a circular formation that surrounded the large faint nuclei of neuronal cells; this gave a good indication during the initial counting process. Only the nucleus of neuronal cells were counted.

The images (Fig.1) show TLR7 to be strictly neuronal, although not all neuronal cells expressed TLR7. Only the neuronal bodies that stained brightly were analysed, among which only the cell profiles with a prominent nucleus was included in the count. Lightly stained cell profiles with a nucleus, or brightly stained cell profiles with no nucleus were neglected. Axons running across the tissue sections around the cell bodies were also observed to express TLR7. Quantitative analysis found that TLR7 was expressed by 18.06% and 19.7% of the total number of sensory neurons in the TG and DRG, respectively. There was no significant difference between the TLR7 expressing population in the TG and DRG (p-value= 0.082, independent t-test).

Qualitative comparison of TLR7 co-expression with neurochemical markers in TG and DRG

An indirect dual-labelling immunohistochemistry was used to indicate the degree of co-expression of TLR7 with its neurochemical markers NF200 and IB4 within the TG and DRG. Each indicating a specific functional sensory neuronal sub-population within the two examined tissue sections. Co-expression of TLR7 in the TG (Fig.2) was then compared to that of the DRG (Fig. 3).

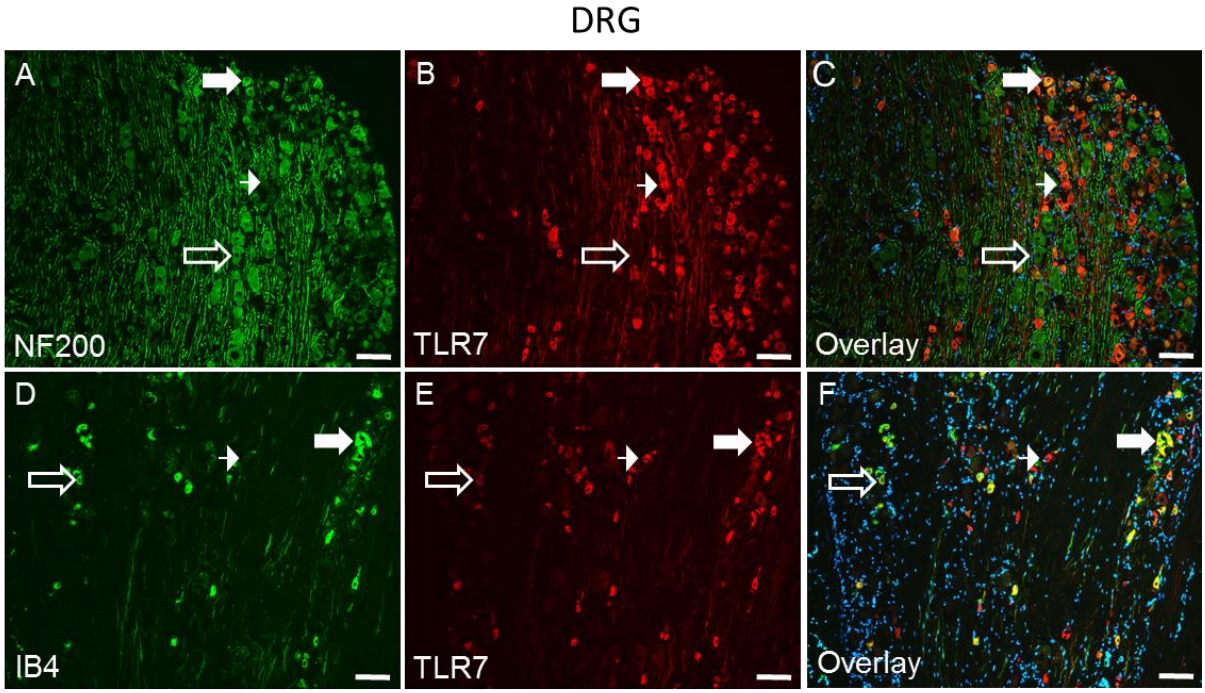

Fig. 2. Fluorescence micrograph of a rat TG double labelled for either NF200-IR (green, A) or IB4-IR (green, D) with TLR7-IR (red, B, E). The overlaid images show minimal co-localization of TLR7-IR with its respective neurochemical markers (yellow; C, F). A large proportion of NF200-IR or IB4-IR neurones do not co-express TLR7-IR (open arrows). A large proportion of TLR7-IR do not co-express NF200-IR or IB4-IR (thin arrows). Minimal co-localisation seen between TLR7-IR and NF200-IR or IB4-IR (filled arrows). Scale bar 100µm

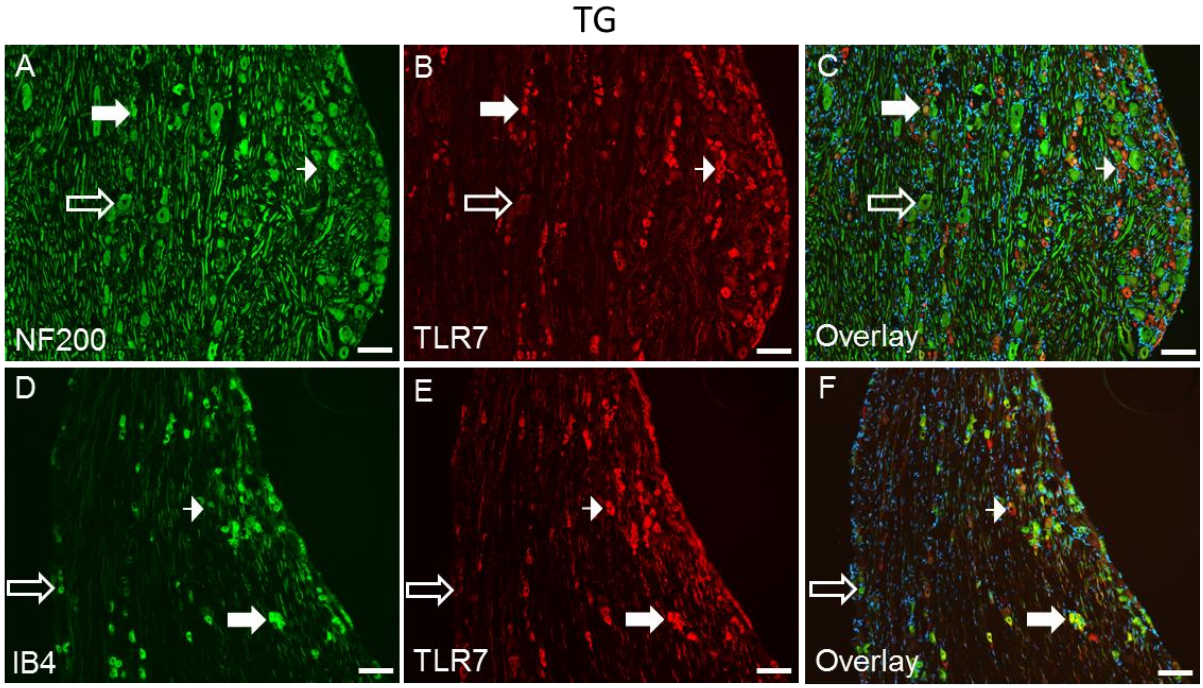

Fig. 3. Fluorescence micrograph of a rat DRG double labelled for either NF200-IR (green, A) or IB4-IR (green, D) with TLR7-IR (red, B, E). The overlaid images show minimal co-localization of TLR7-IR with respective neurochemical markers (yellow; C, F). A large proportion of NF200-IR or IB4-IR neurones do not co-express TLR7-IR (open arrows). A large proportion of TLR7-IR do not co-express NF200-IR or IB4-IR (thin arrows). Minimal co-localisation seen between TLR7-IR and NF200-IR or IB4-IR (filled arrows). Scale bar 100µm.

The tissue samples of both TG **(**Fig. 2) and DRG (Fig. 3**)** showed very similar staining patterns in the distribution and expression of TLR7 with its co-expression to their neurochemical markers, which were all strictly neuronal. Large profiled sensory neurones were seen to express NF200 (Fig. 2A, 3A), whereas TLR7 was shown to be expressed by smaller sensory neurones, although not all small profile sensory neurones were seen to express TLR7 (Fig. 2B, 3B). Very minimal co-expression was seen between TLR7 and NF200 (Fig. 2C, 3C). On the other hand, IB4 was shown to be expressed by the remaining smaller sensory neurones that did not express TLR7 (Fig. 2D, 3D), and no co-expression was seen within larger sensory neurones that expressed NF200. More co-localisation was seen with TLR7 and IB4, than with TLR7 and NF200, this is due to the fact that NF200 is expressed in large cell profiles, but both TLR7 and IB4 are expressed in small cell profiles, which give a higher chance of co-localisation with cells that express TLR7 and cells that express IB4 (Fig. 2F, 3F). What also came to attention was the fact that TLR7 and NF200 in both tissue sections were strongly expressed in neuronal axons running across and around the cell profiles, while IB4 was seen to be expressed very lightly.

Only the neuronal bodies that were brightly stained with the fluorescent marker and showed strong expression of TLR7, NF200 and IB4 were analysed. Among these, only the cell profiles with a prominent nucleus were included in the count. Lightly stained cell profiles containing a nucleus, or brightly stained cell profiles with no nucleus were neglected.

Quantitative comparison of TLR7 co-expression with neurochemical markers in TG and DRG

Qualitative data of the expression and co-expression of TLR7 with neurochemical markers within the TG and DRG, were further analysed quantitatively. Stacked bar charts were used to determine the percentage co-expression of NF200 and IB4 expressing cells within the total number of TLR7 expressing cells (Graph. 1) and the percentage co-expression of TLR7 expressing cells within the total number of NF200 and IB4 expressing cells (Graph. 2)

Graph 1. Stacked bar chart showing the percentage of NF200 and IB4 expressing cells within the total number of TLR7 expressing cells within the TG and DRG, assuming that TLR7 is expressed by 100% of cells.

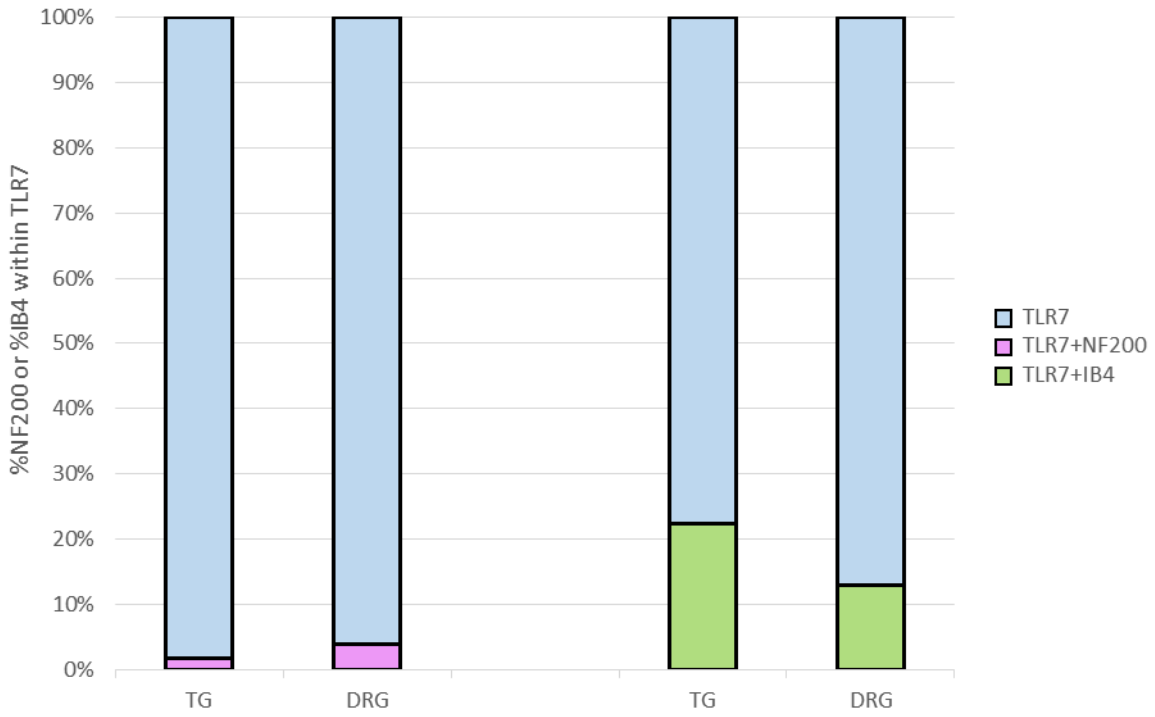

Quantitative analysis showed that, within the total number of sensory neurons that expressed TLR7, only 1.71% and 4.02% co-expressed NF200 in the TG and DRG, respectively. Meanwhile, 23.75% and 14.83% co-expressed IB4 in the TG and DRG, respectively (Graph 1). On the other hand, within the total number of sensory neurons that expressed NF200, only 2.59% and 5.71% co-expressed TLR7 in the TG and DRG, respectively. Meanwhile, within the total number of sensory neurons expressing IB4, 26.76% and 21.91% co-expressed TLR7 in the TG and DRG, respectively (Graph 2). These data showed significant difference between the co-expression of TLR7 expressing cells and NF200 or IB4 expressing cells, but showed no significant difference between the co-expression across both tissue samples. Regardless of the tissue types, both graphs (Graph 1 and 2) showed more co-expression between TLR7 and IB4 expressing cells than the co-expression between TLR7 and NF200 expressing cells, which proves the results of the qualitative analysis. Nevertheless, the qualitative and quantitative data still proves that only a small proportion of co-expression is present between TLR7 expressing cells and NF200 or IB4 expressing cells. These proteins are therefore expressed virtually mutually exclusive of each other.

Graph 2. Stacked bar chart showing the percentage of TLR7 expressing cells within the total number of NF200 or IB4 expressing cells within the TG and the DRG, assuming that TLR7 is expressed by 100% of cells.

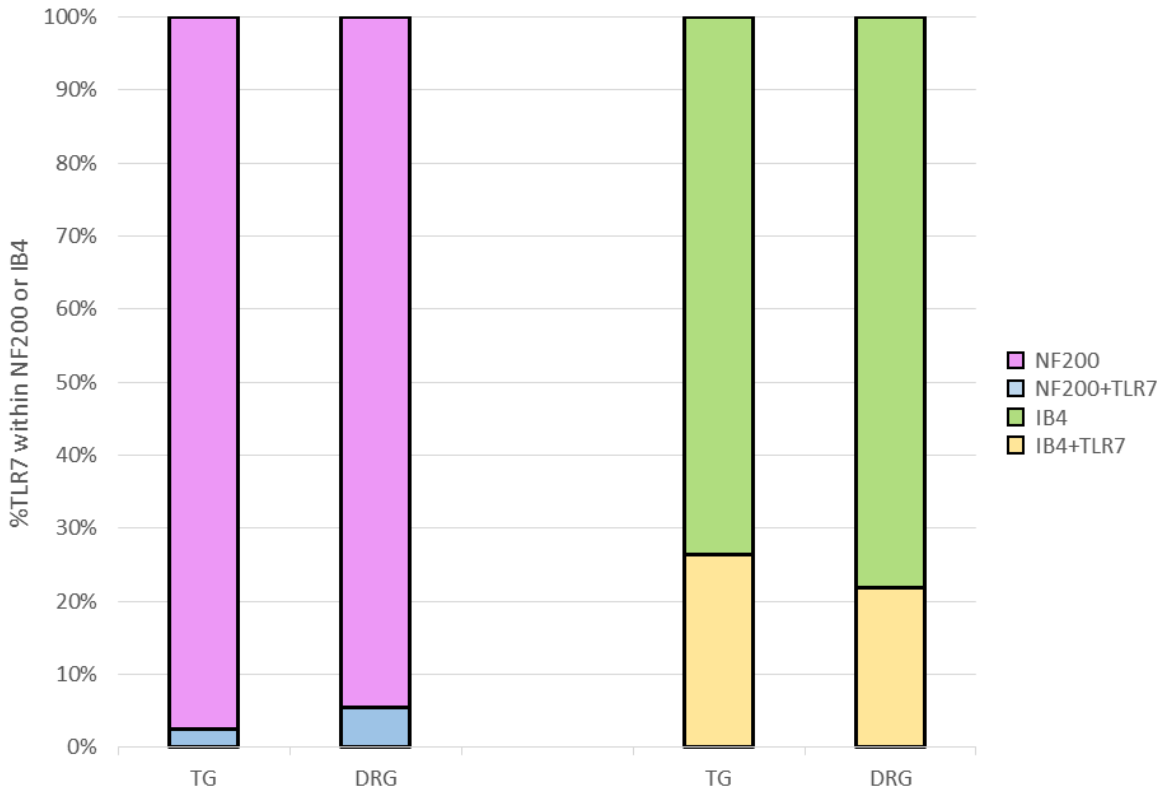

Tongue

Indirect dual-labelling immunohistochemistry was used to characterize the expression of TLR7 in one of the peripheral innervation targets, the tongue (Fig. 4), revealing nerve bundles with unique identification of each axon.

Small to medium sized cross section of nerve bundles were predominantly seen in the tongue (Fig. 4A). The small nerve bundles contained similar sized axons that were uniformly distributed across the profile of the nerve bundle (Fig. 4B). These small axons were shown to all express NF200 only, with no TLR7 expression. No co-localization of NF200 and TLR7 expression was determined either. However, the medium to large nerve bundles contained axons with a variety of shapes and sizes, which were seen to be distributed irregularly throughout the nerve bundle (Fig. 4C). These medium to large bundles were seen to contain axons that expressed only NF200, only TLR7 and both. A detailed expression and co-localization of neurochemical markers in the tongue are shown in Fig. 5 and 6. Interestingly, the cross sectional nerve bundles were only seen around a single large duct, which was only found on the lateral borders of both sides of the tongue (Fig. 4A). Very few longitudinal sections of nerve bundles were seen in the tongue, that were occasionally seen further away from the duct, closer to surface of the tongue (Fig. 6).

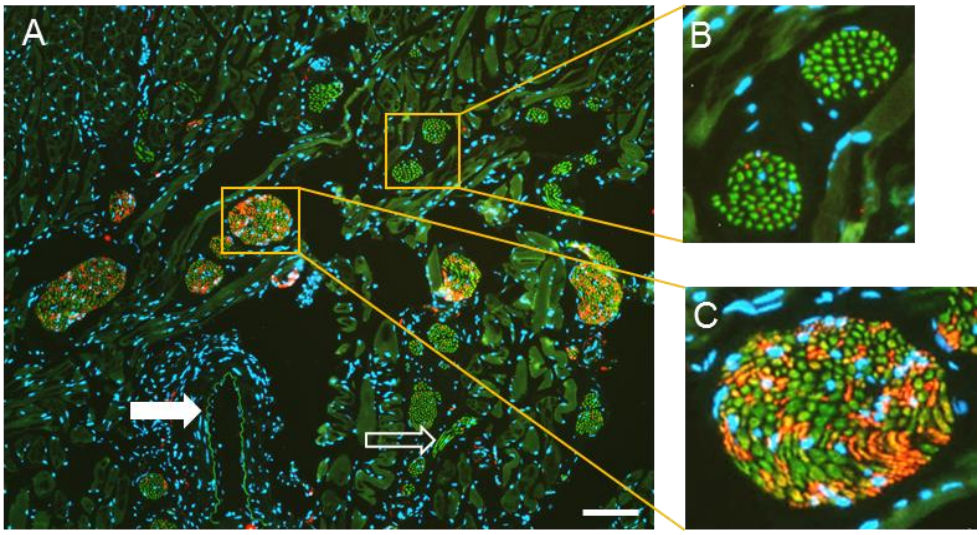

Fig. 4. Fluorescence micrograph of a transverse section of a rat tongue, double labelled for NF200-IR (green) with TLR7-IR (red). Small to large transverse sections of nerve bundles seen in the tongue (A), these nerve bundles are magnified in images B and C respectively showing neurochemical expression well as co-expression between TLR7 and NF200 expressing axons (yellow, C). A longitudinal section of nerve bundles are seen (open arrow), as well as a large duct with NF200-IR expressing membrane (filled arrows). Scale bar 100µm.

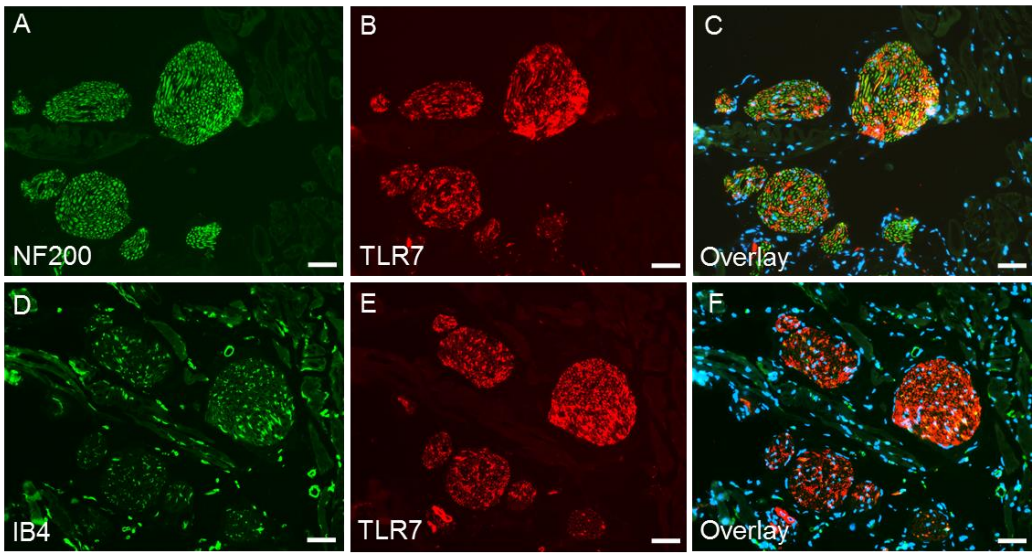

Fig. 5. Fluorescence micrograph of a rat tongue double labelled for either NF200-IR (green, A) or IB4-IR (green, B) with TLR7-IR (red, B, E). Images show cross-sectional neuronal bundles containing individually stained axons. Overplayed images show minimal co-localization of TLR7-IR with respective neurochemical markers (yellow; C, F). Scale bar 50µm.

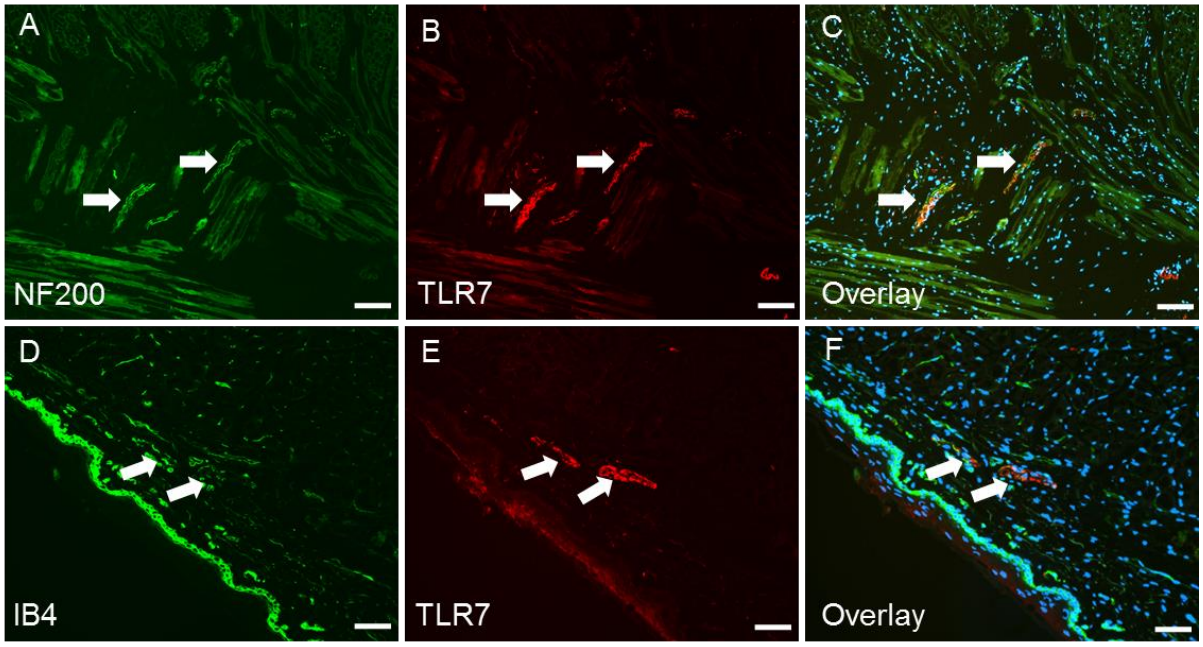

Fig. 6. Fluorescence micrograph of a rat tongue double labelled for either NF200-IR (green, A) or IB4-IR (green, B) with TLR7-IR (red, B, E). Images show longitudinal neuronal bundles containing individually stained axons. Overplayed images show minimal co-localization of TLR7-IR with respective neurochemical markers (yellow; C, F). Scale bar 50µm.

A range of small to large cross sectional profiles of nerve bundles were seen **(**Fig. 5) that contained large numbers of axons. A large proportion of these axons were seen to express NF200 (Fig. 5A). Axons that are not expressing NF200 were seen to express TLR7 (Fig. 5 B, E), although the smaller nerve bundles were predominantly seen to express NF200 with little to no TLR7 expression. Very minimal co-expression was seen between NF200 expressing axons and TLR7 expressing axons **(**Fig. 5C). Meanwhile, very few axons are seen to be expressing IB4 (Fig. 5D), compared to the amount of NF200 and TLR7 expressing axons. Very minimal co-expression is also seen between the IB4 expressing axons and the TLR7 expressing axons (Fig. 5F).

The longitudinal cross-section of the nerve bundles however, were seen to contain very few axons (Fig. 6) which were located close to the epithelial layers of the tongue that clearly expressed NF200 and IB4 (epithelial layer not shown in images A, B and C) forming dense wave-like appearance. Much like the large cross sectional profiles of the nerve bundles, individual axons within the longitudinal cross sections of nerve bundles were shown to express NF200 (Fig. 6A) and TLR7 (Fig. 6B, E), although very few axons were seen to express IB4 (Fig. 6D). Image overlay showed very minimal co-expression between NF200 and TLR7 expressing cells in the axons (Fig. 6C) but showed even less co-expression between IB4 and TLR7 expressing cells (Fig. 6F).

Discussion

TLR7 distribution within TG and DRG

Various neuronal sub-populations were distinguished in this study using well known neurochemical markers that allowed the differentiation between TLR7 expressing cells and non-TLR7 expressing cells through the process of elimination.

Nociceptors are divided into two major classes. The first class includes a small population of myelinated A-fibre afferents, which were seen to be expressed by NF200 in the neuronal cell bodies of the TG and DRG. NF200 is a known marker of myelinated A-fibre neurons (Kobayashi et al., 2005) as they are involved almost exclusively in the distinction of the NF-positive neuronal population (Basbaum et al., 2009). These myelinated A-fibre afferents include high threshold medium diameter (600 –1,200 μm^2) Aδ afferents, known to mediate acute sharp or "first" pain that have an association with the application of intense heat or sharp objects on the skin. As well as rapidly conducting, of low threshold and large diameter (>1,200 μm^2) Aβ fibres that are known to respond to innocuous mechanical stimulation of light touch. Aδ nociceptors further subdivide into two main classes; the first class being Type I high threshold mechanical nociceptors, that have relatively high heat threshold of over 50°C, and respond to both chemical and mechanical stimuli. The second class being Type II Aδ nociceptors that have a very high mechanical threshold, but a much lower heat threshold, (Woolf and Ma, 2007; Dong et al., 2001). These NF200 expressing cells are found in 46.8%+-3.8% of the total neuronal profiles (Bennet et al., 1998; Woolf and Ma, 2007). This correlates to the qualitative analysis in this paper, which has suggested the expression of NF200 in almost half of the neuronal cell population in the TG and the DRG, seen in medium to large profile sized neurons that are known to only be expressed by NF200.

The remaining neuronal cell population that had not been expressed by NF200, was seen to be expressed by the second class of nociceptors of which almost half expressed TLR7 and the other half expressed IB4. This second class of nociceptors are small diameter (<600 μm^2) unmyelinated C-fibres that convey slow or "second" pain and are responsible for the burning nociceptive sensation detected from noxious heat stimuli, and from prolonged mechanical stimuli. They are populations of relatively small and medium-sized neurons (Kobayashi et al., 2005) that are exclusive to the NF200-expressing population of neurons. Similarly, much like the myelinated afferents, the unmyelinated C-fibres include a population of both mechanical and heat sensitive nociceptors, allowing them to respond to multiple forms of pruritic stimuli. However, not all C-fibres are nociceptors, instead of responding to chemical or heat stimulation, some unmyelinated afferent population respond to cooling, whereas others appear to mediate pleasant touch such as an innocuous stroking of a skin or a hair on the skin (Olausson et al., 2007; Basbaum et al., 2009).

The heterogeneity of C-fibre nociceptors have further been classified into peptidergic and non-peptidergic cells. Firstly, peptidergic populations of C-fibres nociceptors express tyrosine kinase receptor A(TrkA), that are nerve growth factor (NGF) dependent; also releasing calcitonin-gene related peptide (CGRP), substance P (SP) and neuropeptides. In addition, peptidergic cells express the transient receptor potential V1 (TRPV1) ion channel that is known to be activated by noxious heat stimuli. TRPV1 functions as the receptor for capsaicin, which is the pungent ingredient in chili peppers (Bautista et al., 2006; Patapoutian, Tate and Woolf, 2009; Story et al., 2003). As well as TRPA1 ion channels that can be activated by iisothiocyanate or thiosulfinate compounds which are compounds of the pungent ingredients of mustard oil and garlic, respectively (Patapoutian, Tate and Woolf, 2009). In addition to TLR7 being coupled to TRPA1 and TRPV1, they play an important role in the detection of extracellular microRNAs (miRNA) which result in the excitation of nociceptors (Basbaum et al.,

2009; Woolf and Ma, 2007). These nociceptors were visibly seen in the results of this study, expressed by almost half of the small diameter cells within the TG and DRG.

Secondly, C-fibre nociceptors include non-peptidergic populations that express c-Ret neurotrophin receptors which are targeted by glial-derived neurotrophic factor (GDNF), and P2X3 that is thought to mediate pain-inducing actions of ATP, as well as artemin, neuturin. IB4 is known to exclusively bind to neurons with unmyelinated axons, a large population of this is bound to non-peptidergic C-fibre nociceptors (53–63%) (Stucky and Lewin, 1999; Dong et al., 2001). This proves the results in this study, whereby IB4 expressing cells were taken over by almost half of the C-fibre nociceptors. Nevertheless, IB4 occasionally shows binding to CGRP and substance P-expressing cells (Molliver et al., 1997; Bennet et al., 1998) resulting in co-expression of IB4 and TLR7 binding populations (Stucky and Lewin, 1999; Woolf and Ma, 2007). This has shown that almost 18% of TLR7 cells also bind to IB4, which correlates with this study's results, whereby IB4 was shown to be expressed by 23.75% and 14.83% of TLR7 in the TG and DRG, respectively. Results of this study have indicated that 26.76% and 21.91% of IB4 expressing cells in the TG and DRG also express TLR7, correlating to studies that show that almost 25% of IB4 cells also express TLR7 (Bennet et al., 1998).

Although the studies above have shown that TLR7 is expressed by almost 30% and 30%-50% of the total cell population in the TG and DRG respectively, the results in this study indicate a much lower number of 18.6% and 19.7% in the TG and DRG, respectively. This may be explained by a study conducted by Bennet et al. (1998) which investigated the expression of GDNF receptors within adult sensory neurons using exogenous trophic factors. Bennett and colleagues showed a downregulation of C-fibre nociceptors after 2 weeks of axotomy that also led to the loss in the sensitivity of neurochemical markers, further giving evidence of a decrease in the percentage population binding to IB4 from 40% to 20% thereby potentially explaining the low numbers detected in our study. However, it may be unlikely since the present study was conducted on intact animals. Therefore, further research is needed for an explanation of the lower numbers shown in this study. In addition, Bennet et al. (1998) has shown that a small number of TLR7 expressing cells also expressed NF200, which ranged from 18-28% of total TLR7 profiles in the DRG. However, this study has showed a significantly lower number of 4% and 2% in the TG and DRG respectively. These low results may also be explained by the study done by Bennet et al. (1998), who has further expanded on this by showing that GDNF reduced axotomy-induced changes in IB4 expressing cells, therefore suggesting a potential area for further study.

The variation of data in our study compared to others may have also been due to individual techniques in counting the cells. Many studies did not give an indication of the mean fluorescence intensity unit that was used to set the threshold for positive counting for each antibody. Determining expression and co-localization through a set approach would have given more accurate data, in addition to a more accurate comparison between studies.

The TG and DRG do not only contain the bodies of nociceptors, but also contain a large number of satellite glial cells and Schwann cells. The satellite glial cells are the main glial cells in the sensory ganglia, alongside the Schwann cells. Each sensory neuron is entirely surrounded by satellite glial cells coupled with gap junctions, forming a myelin sheath around the cell body which provides a possible explanation of the

observation seen at the initial stage while counting the neuronal cell nuclei. The Schwann cells, on the other hand, are the principal glia of the peripheral nervous system and are involved in the crucial maintenance and the survival of the neurones and wrap around small diameter C-fibre nociceptors. DAPI is a nucleic acid fluorescent stain that is also characterized to give variant staining densities according to the size of the nucleus (Zhao et al., 2010; Kapuscinski, 1995; Griffin and Thompson, 2008; Pannese et al., 2003). This gives a reason as to why the nuclei of satellite cells and Schwann cells were able to take up DAPI and emit a very bright blue fluorescent staining, whereas the nuclei of neuronal cells were very faint in colour.

Tongue

The tongue is a very intricate organ (Zur, Mu and Sanders, 2004) that plays an important role in the biological activities of tasting, manipulating food during mastication and the act of swallowing, as well as dilating the airway during respiration and shaping the sounds of speech in humans (Saigusa et al., 2006). It is known that the tongue is composed of intrinsic muscles that include superior and inferior, transverse and vertical muscles, as well as extrinsic muscles that include hypoglossus, styloglossus, genioglossus, and palatoglossus muscles (Mu and Sanders, 1999). The tongue is known to be innervated by four cranial nerves; the glossopharyngeal nerve (CN IX) that provides the posterior one-third of the tongue mucosa with taste and general sensation (Stutley, Cooke and Parsons, 1989; Lawn, 1966; Yamamoto, 1975), the hypoglossal nerve (CN XII) that provides the muscles of the tongue with motor supply (McClung and Goldberg, 2000; Mu and Sanders, 1999), the lingual branch of the mandibular division from the trigeminal nerves (CN V) that is responsible for the supply of primary afferent fibres to the anterior two-thirds of the tongue (Heasman and Beynon, 1986), and the chorda tympani branch of the facial nerve (CN VII) that is responsible for the transmission of taste afferents from the mucous membranes of the tongue and convey secretomotor efferents to the submandimbular and sublingual salivary glands (Gritzmann and Fruhwald, 1988; Zur, Mu and Sanders, 2004). The diameter of the main trunks of the three major nerves are ranked as lingual, hypoglossal, glossopharyngeal, from biggest to smallest (McClung and Goldberg, 2000; Mu and Sanders, 1999; Carrión et al., 2015).

Previous studies have shown that the axons and dendrites are known to express NF200, which were seen in sections of smooth and striated muscles and have been localized to 10nm diameter filaments (Trojanowski, Walkenstein and Lee, 1986; Carrión et al., 2015). However, this study is the first to look into a selected facial innervation target, specifically the tongue, where the TLR7 was seen to remarkably be expressed in the nerves of the tongue.

The lingual nerve enters the tongue laterally with the lingual artery, through the ventral mucosa of the tongue, into the lesions between the genioglossus muscle and the inferior longitudinal muscle, which is located anterior to the circumvallate papillae. The lingual nerve then splits into two branches, first the lateral, then the medial branches, which act to innervate the anterior thirds and the middle of the tongue, respectively. The lateral and medial branches are restricted to the ventrolateral tongue mucosa, and are connected to the hypoglossal nerve. The lingual nerve courses its way anteriorly along the lateral border of the tongue, and provides bilateral innervation to the anterior parts of the tongue, but very few of the nerves are distributed to the medial anterior two-thirds of the tongue. The sensory innervation of the tongue was shown to be concentrated near the lateral edge of the tongue (Zur, Mu and Sanders, 2004;

Saigusa et al., 2006). In the human tongue, the average diameter of the main trunk of the lingual nerve is found to be 3.5mm, this is then split into axonal bundles of about 1mm in diameter, which further subdivides into axons of 0.5-0.75mm diameter. The interconnection between the lingual nerve and the hypoglossal nerve is approximately 0.25mm apart. The nerve bundles become smaller further anteriorly down the tongue. The size of the nerves differ among different species, but the average size proportion between the nerves are similar. The hypoglossal nerve enters more medially between the lingual and glossopharyngeal nerve that enters posteromedially and innervates the posterior of the tongue. (Zur, Mu and Sanders, 2004). The hypoglossal nerve subdivides into lateral and medial branches and further branches out at the level of the circumvallate papillae, anteriorly continuing to innervate both the transverse and vertical muscles in the anterior two-thirds of the tongue (McClung and Goldberg, 2000; Mu and Sanders, 1999).

The tongue used in this study was diagonally dissected at the medial region where the tongue meets the floor of the mouth. This section does not contain circumvallate papillae of the glossopharyngeal nerve, hence, no nerve bundles were seen around the middle of the transversely cut tissue section. Nerve bundles were only seen at the inferior medial lateral region on both sides of the tongue, with visible small to large nerve bundles, suggesting that the large bundles belong to the lingual nerve and the small bundles belong to the hypoglossal nerve. This is anatomically explained as the lingual nerve enters the tongue anteriorly to the hypoglossal nerve and retains large nerve bundles throughout the medial of the tongue, it only splits off into small bundles once it reaches the anterior lesion of the tongue. Whereas, the hypoglossal nerve splits into small bundles at the level where the lingual nerve enters the tongue. This anatomical explanation is further proven by the immunohistochemistry. The smaller nerves do not express TLR7, but do express NF200, In addition, the individual nerve fibres are seen to have equal sized diameters and uniformly distributed throughout the nerve bundle, confirming that these structures are hypoglossal motor nerves**.**

On the other hand, the larger nerve bundles do express TLR7 as well as NF200 and IB4, also giving off a few co-expressed fibres. It is generally accepted that the lingual nerve is a sensory nerve which mediates sensation to the anterior two-thirds of the tongue; however, studies have shown that the motor root of the trigeminal nerve supplies its motor fibres which travels into the lingual branch and into the inferior longitudinal muscles (Fitzgerald and Law, 1958; Saigusa et al., 2006; Zur, Mu and Sanders, 2004; Carrión et al., 2015; Mu and Sanders, 2010). This explains the irregular distribution of unequal sized fibres within the nerve bundle, as motor nerves have a bigger cell body and give off bigger axons, whereas the sensory neurones have smaller cell bodies and gives off smaller axons. This shoes that the subclasses are divided into large diameter A-fibre low-threshold mechanoreceptors expressing NF200, and small diameter C-fibre high-threshold nociceptors expressing TLR7 and IB4.

The tongue also contains several arteries and veins, including the lingual artery that is originated from the external carotid artery and takes its course along the medial side of the hypoglossus muscle; as well as the sublingual artery that takes its course in a forward direction between the sublingual gland and the genioglossus muscle. The deep lingual artery is located at the side of the genioglossus muscle, which slopes in an arch towards the dorsum of the tongue (Hellstrand, 1981). Some arteries were seen around the nerve bundles (not shown in selected images).

The large nerve bundles were seen to be surrounding a single large duct in any given tissue section observed. NF200 and IB4 are also known to be used histochemically for specifically labelling endothelial cells in a number of species (Binch et al., 2015; Stucky and Lewin, 1999), confirming that the structures surrounded by the nerve bundles were ducts and not blood vessels. The tongue contains three distinct sets of minor salivary glands with its ducts throughout the tongue; this includes the glands of Bladin and Nuhn, the glands of Weber, and the glands of Von Ebner. The glands of Bladin and Nuhn are serous and mixed mucous glands that are embedded within the musculature of the anterior tongue ventrum. The intercalated ducts consist of simple cuboidal epithelium and merge with excretory duct lined with columnar cells. The glands of Von Ebner are pure serous glands which drain through small ducts into the base of the grooves that surround the circumvallate papillae and the base of the cleft between the foliate papillae. The glands of weber are pure mucous glands, they are abundant along the lateral border of the tongue and open into the crypts of the lingual tonsils on the posterior tongue dorsum (Sugerman, Savage and Young, 2000). The origin of the duct is unknown due to very limited information of its anatomy within the tongue, hence, further research is needed for confirmation of the identity of the duct.

There are longitudinal nerve fibres that are occasionally seen in the tissue sections, around the area where the nerve bundles are found, as well as around the edges of the tongue tissues near the epithelial layers of the tongue. This would be due to the anatomy of the nerves, as the tongue sections were cut transversely right where the lingual nerve entered the tongue, suggesting that the lingual nerve would still be intact in large bundles without yet being subdivided. Whereas the hypoglossal nerve enters more posteriorly to the lingual nerve, and starts to divide at the point where the lingual nerve enters the tongue, this would explain the visible small bundles which are most probably hypoglossal nerves, and the larger bundles which are most probably lingual nerves. If the sections were to be transversely cut around the anterior region of the tongue, both the lingual and the hypoglossal nerves would be seen to have smaller diameters compared to the medial region of the tongue. In addition, a dense number of longitudinal sections of the nerves amongst the chorda tympani branches of the facial nerves are expected to be seen, as the nerves branch off and innervate different muscles and areas of the anterior of the tongue. This theory is yet to be confirmed with more experiments.

As mentioned previously, nociceptors in the TG and the DRG express TLR7 which are coupled to various molecules such as TRPA1 ion channel which is activated by compounds found in ingredients such as mustard oil and garlic, and TRPV1 ion channel which is activated by compounds in chili as well as mediating itch. Topical application of these agents have long been known to excite sensory nerve fibres, thereby producing acute pain and neurogenic inflammation. This may suggest an important role of the tongue, as the nerves in the tongue may detect such molecules and compounds of specific ingredients, distinguishing different sensations and reacting accordingly by sending signals to the brain and spinal cord.

Therapeutic targets using TLR7

An afterthought connected with this study leads to recent studies that have demonstrated increased data involving TLRs in the pathogenesis of Alzheimer's disease, giving evidence for the upregulation of TLRs, and the expression of increased levels of TLR7 in transgenic mice. In addition, an elevation in mRNA levels for TLR7 in plaque-associated microglia had been exhibited, suggesting that TLR7 activation

may lead to glial cell activity being modulated in patients with Alzheimer's disease (Trudler, Farfara and Frenkel, 2010). Other studies have suggested TLR7 involvement in pro-inflammatory responses of microglia, which may have an association with neurotoxicity, as well as the involvement of microglia in the pathogenesis Amyotrophic lateral sclerosis, leading to TLR7 elevation (Trudler, Farfara and Frenkel, 2010)**.** TLR7 showed a protective immunity for hepatitis virus B and C, by the mediation of an endogenous type I IFN response, which may lead to the eradication of specific hepatitis virus. Furthermore, studies have suggested that TLR7 agonists may be used in adjuvant therapies to accelerate the process of immune reconstitution (Funk et al., 2014; McGilvray et al., 2012). Interestingly, studies have shown an important role of the activation of TLR7 in the immune responses against early plasmodial infections (Baccarella et al., 2013).

Studies in the trigeminal system has exhibited the association of TLR7 expression with tumour grade, showing significantly elevated levels of TLR7 in the oral squamous cell carcinoma of the tongue. This may lead to alternative therapeutic approaches in treatment of neurologically associated diseases (Pakdel et al., 2015).

Conclusion

There is a growing body of evidence suggesting that TLR7 and its expression in nociceptors are crucial factors in mediating nociception and neuro-immune signalling. The results in this paper fully support the mechanism by which nociceptors work independently of the innate immune activation by directly detecting and responding to pathogenic challenges. While there are a few studies that looked into the TLR7 expression in the DRG, only one other study has looked into the expression of TLR7 distribution in the TG and its co-expression with other neurochemical markers. Therefore, more research is needed to confirm the quantitative analysis of the expression and distribution, as well as effectively identifying the individual axons and their roles in the transmission of signals from the innervation targets of the PNS to the CNS. The discovery of TLR7 expression in the individual axons of the tongue is suggestive of the role the tongue plays in the detection of various harmful molecules and substances including infectious pathogens, particularly viruses. This study has also allowed the identification of each axon, suggests that TLR7 may play an important role in initiating defence mechanisms throughout the body, which may represent a base line for direct nociceptive therapeutic targets in the future through individually marked axons. This not only provides an essential tool for the study of nociceptive mechanisms, but also contributes to the study of various other innervation targets within the body, thereby highlighting the importance of further research into the innovation of nerves and the detection of TLR7.

Author contributions

Sara Kawamura and Dr. Stephen W. N. Thompson developed and designed this study. Dr. Stephen W. N. Thompson conducted the home office schedule 1 procedure. Sara Kawamura and Dr. Joceline Triner prepared the solutions and Sara Kawamura conducted the experiments, collected the analysis and critically revised the manuscript for final approval.

Acknowledgements

I would like to thank Dr. Stephen W. N. Thompson for his guidance and constant support throughout this study, as well as Dr. Joceline Triner for her assistance in the running of the experiments and daily encouragement. This project was supported by

Plymouth University Faculty of Biomedical and Healthcare Sciences, as well as Peninsula Schools of Medicine and Dentistry, who have provided the necessary equipment and the use of their facilities throughout the duration of this study.

References

Baccarella, A., Fontana, M., Chen, E. and Kim, C. (2013). Toll-Like Receptor 7 Mediates Early Innate Immune Responses to Malaria. *Infection and Immunity*, 81(12), pp.4431-4442.

Barajon, I., Serrao, G., Arnaboldi, F., Opizzi, E., Ripamonti, G., Balsari, A. and Rumio, C. (2009). Toll-like Receptors 3, 4, and 7 Are Expressed in the Enteric Nervous System and Dorsal Root Ganglia. *Journal of Histochemistry & Cytochemistry*, 57(11), pp.1013-1023.

Basbaum, A., Bautista, D., Scherrer, G. and Julius, D. (2009). Cellular and Molecular Mechanisms of Pain. *Cell*, 139(2), pp.267-284.

Bautista, D., Jordt, S., Nikai, T., Tsuruda, P., Read, A., Poblete, J., Yamoah, E., Basbaum, A. and Julius, D. (2006). TRPA1 Mediates the Inflammatory Actions of Environmental Irritants and Proalgesic Agents. *Cell*, 124(6), pp.1269-1282.

Bennet, D., Michael, G., Ramachandran, N., Munson, J., Averill, S., Yan, Q., McMahon, S. and Priestley, J. (1998). A Distinct Subgroup pf Small DRG Cells Express GDNF Receptor Components and GDNF Is Protective for These Neurons after Nerve Injury. *The journal of Neuroscience*, 18(8), pp.3059-3072.

Binch, A., Cole, A., Breakwell, L., Michael, A., Chiverton, N., Creemers, L., Cross, A. and Le Maitre, C. (2015). Nerves are more abundant than blood vessels in the degenerate human intervertebral disc. *Arthritis Research & Therapy*, 17(1).

Bsibsi, M., Ravid, R., Gveric, D. and van Noort, J. (2002). Broad Expression of Toll-Like Receptors in the Human Central Nervous System. *Journal of Neuropathology & Experimental Neurology*, 61(11), pp.1013-1021.

Cameron, J., Alexopoulou, L., Sloane, J., DiBernardo, A., Ma, Y., Kosaras, B., Flavell, R., Strittmatter, S., Volpe, J., Sidman, R. and Vartanian, T. (2007). Toll-Like Receptor 3 Is a Potent Negative Regulator of Axonal Growth in Mammals. *Journal of Neuroscience*, 27(47), pp.13033-13041.

Carrión, D., Korkmaz, Y., Cho, B., Kopp, M., Bloch, W., Addicks, K. and Niedermeier, W. (2015). Loss of Aβ-nerve endings associated with the Merkel cell-neurite complex in the lesional oral mucosa epithelium of lichen planus and hyperkeratosis. *International Journal of Oral Science*, 8(1), pp.32-38.

Dong, X., Han, S., Zylka, M., Simon, M. and Anderson, D. (2001). A Diverse Family of GPCRs Expressed in Specific Subsets of Nociceptive Sensory Neurons. *Cell*, 106(5), pp.619-632.

Du, X., Poltorak, A., Wei, Y. and Beutler, B. (2000). Three novel mammalian toll-like receptors: gene structure, expression, and evolution. *European Cytokine Network*, 11(3), pp.362-71.

Fitzgerald, M. and Law, M. (1958). The peripheral connexions between the lingual and hypoglossal nerves. *Journal of Anatomy*, 92(2), pp.178-188.

Funk, E., Kottilil, S., Gilliam, B. and Talwani, R. (2014). Tickling the TLR7 to cure viral hepatitis. *Journal of Translational Medicine*, 12(1), p.129.

Griffin, J. and Thompson, W. (2008). Biology and pathology of nonmyelinating Schwann cells. *Glia*, 56(14), pp.1518-1531.

Gritzmann, N. and Fruhwald, F. (1988). Sonographic anatomy of tongue and floor of the mouth. *Dysphagia*, 2(4), pp.196-202.

Hashimoto, C., Hudson, K. and Anderson, K. (1988). The Toll gene of drosophila, required for dorsal-ventral embryonic polarity, appears to encode a transmembrane protein. *Cell*, 52(2), pp.269-279.

Heasman, P. and Beynon, A. (1986). Quantitative Diameter Analysis of Lingual Nerve Axons in Man. *Journal of Dental Research*, 65(7), pp.1016-1019.

Helley, M., Abate, W., Jackson, S., Bennett, J. and Thompson, S. (2015). The expression of Toll-like receptor 4, 7 and co-receptors in neurochemical sub-populations of rat trigeminal ganglion sensory neurons. *Neuroscience*, 310, pp.686-698.

Hellstrand, E. (1981). Contraction times of the cat's tongue muscles measured by light reflection. Innervation of individual tongue muscles. *Acta Physiologica Scandinavica*, 111(4), pp.417-423.

Imai, Y., Kuba, K., Neely, G., Yaghubian-Malhami, R., Perkmann, T., van Loo, G., Ermolaeva, M., Veldhuizen, R., Leung, Y., Wang, H., Liu, H., Sun, Y., Pasparakis, M., Kopf, M., Mech, C., Bavari, S., Peiris, J., Slutsky, A., Akira, S., Hultqvist, M., Holmdahl, R., Nicholls, J., Jiang, C., Binder, C. and Penninger, J. (2008). Identification of Oxidative Stress and Toll-like Receptor 4 Signaling as a Key Pathway of Acute Lung Injury. *Cell*, 133(2), pp.235-249.

Iwasaki, A. and Medzhitov, R. (2004). Toll-like receptor control of the adaptive immune responses. *Nature Immunology*, 5(10), pp.987-995.

Iwasaki, A. and Medzhitov, R. (2010). Regulation of Adaptive Immunity by the Innate Immune System. *Science*, 327(5963), pp.291-295.

Kapuscinski, J. (1995). DAPI: a DNA-Specific Fluorescent Probe. *Biotechnic & Histochemistry*, 70(5), pp.220-233.

Kobayashi, K., Fukuoka, T., Obata, K., Yamanaka, H., Dai, Y., Tokunaga, A. and Noguchi, K. (2005). Distinct expression of TRPM8, TRPA1, and TRPV1 mRNAs in rat primary afferent neurons with aδ/c-fibres and colocalization with trk receptors. *The Journal of Comparative Neurology*, 493(4), pp.596-606.

Kumar, H., Kawai, T. and Akira, S. (2009). Pathogen recognition in the innate immune response. *Biochemical Journal*, 420(1), pp.1-16.

Lafon, M., Megret, F., Lafage, M. and Prehaud, C. (2006). The Innate Immune Facet of Brain: Human Neurons Express TLR-3 and Sense Viral dsRNA. *Journal of Molecular Neuroscience*, 29(3), pp.185-194.

Lawn, A. (1966). The localization, in the nucleus ambiguus of the rabbit, of the cells of origin of motor nerve fibres in the glossopharyngeal nerve and various branches of the vagus nerve by means of retrograde degeneration. *The Journal of Comparative Neurology*, 127(2), pp.293-305.

Liu, T., Xu, Z., Park, C., Berta, T. and Ji, R. (2010). Toll-like receptor 7 mediates pruritus. *Nature Neuroscience*, 13(12), pp.1460-1462.

McClung, J. and Goldberg, S. (2000). Functional anatomy of the hypoglossal innervated muscles of the rat tongue: A model for elongation and protrusion of the mammalian tongue. *The Anatomical Record*, 260(4), pp.378-386.

McGilvray, I., Feld, J., Chen, L., Pattullo, V., Guindi, M., Fischer, S., Borozan, I., Xie, G., Selzner, N., Heathcote, E. and Siminovitch, K. (2012). Hepatic Cell–Type Specific Gene Expression Better Predicts HCV Treatment Outcome Than IL28B Genotype. *Gastroenterology*, 142(5), pp.1122-1131.e1.

Midwood, K., Sacre, S., Piccinini, A., Inglis, J., Trebaul, A., Chan, E., Drexler, S., Sofat, N., Kashiwagi, M., Orend, G., Brennan, F. and Foxwell, B. (2009). Tenascin-C is an endogenous activator of Toll-like receptor 4 that is essential for maintaining inflammation in arthritic joint disease. *Nature Medicine*, 15(7), pp.774-780.

Mishra, B., Mishra, P. and Teale, J. (2006). Expression and distribution of Toll - like receptors in the brain during murine neurocysticercosis. *Journal of Neuroimmunology*, 181(1-2), pp.46-56.

Molliver, D., Wright, D., Leitner, M., Parsadanian, A., Doster, K., Wen, D., Yan, Q. and Snider, W. (1997). IB4-Binding DRG Neurons Switch from NGF to GDNF Dependence in Early Postnatal Life. *Neuron*, 19(4), pp.849-861.

Mu, L. and Sanders, I. (1999). Neuromuscular organization of the canine tongue. *The Anatomical Record*, 256(4), pp.412-424.

Mu, L. and Sanders, I. (2010). Human tongue neuroanatomy: Nerve supply and motor endplates. *Clinical Anatomy*, 23(7), pp.777-791.

Olausson, H., Cole, J., Rylander, K., McGlone, F., Lamarre, Y., Wallin, B., Krämer, H., Wessberg, J., Elam, M., Bushnell, M. and Vallbo, Å. (2007). Functional role of unmyelinated tactile afferents in human hairy skin: sympathetic response and perceptual localization. *Experimental Brain Research*, 184(1), pp.135-140.

Pakdel, F., Pouralibaba, F., Pakdel, S., Khiyavi, R., Falsafi, P., Eslami, H., Fakhrzadeh, V. and Kahnamouii, S. (2015). Expression of Toll-like receptors in squamous cell carcinoma of the tongue. *Scholars Research Library*, 7(2), pp.20-24.

Pannese, E., Ledda, M., Cherkas, P., Huang, T. and Hanani, M. (2003). Satellite cell reactions to axon injury of sensory ganglion neurons: Increase in number of gap junctions and formation of bridges connecting previously separate perineuronal sheaths. *Anatomy and Embryology*, 206(5), pp.337-347.

Park, C., Xu, Z., Berta, T., Han, Q., Chen, G., Liu, X. and Ji, R. (2014). Extracellular MicroRNAs Activate Nociceptor Neurons to Elicit Pain via TLR7 and TRPA1. *Neuron*, 82(1), pp.47-54.

Patapoutian, A., Tate, S. and Woolf, C. (2009). Transient receptor potential channels: targeting pain at the source. *Nature Reviews Drug Discovery*, 8(1), pp.55-68.

Qi, J., Buzas, K., Fan, H., Cohen, J., Wang, K., Mont, E., Klinman, D., Oppenheim, J. and Howard, O. (2011). Painful Pathways Induced by TLR Stimulation of Dorsal Root Ganglion Neurons. *The Journal of Immunology*, 186(11), pp.6417-6426.

Roach, J., Glusman, G., Rowen, L., Kaur, A., Purcell, M., Smith, K., Hood, L. and Aderem, A. (2005). The evolution of vertebrate Toll-like receptors. *Proceedings of the National Academy of Sciences*, 102(27), pp.9577-9582.

Saigusa, H., Tanuma, K., Yamashita, K., Saigusa, M. and Niimi, S. (2006). Nerve fiber analysis for the lingual nerve of the human adult subjects. *Surgical and Radiologic Anatomy*, 28(1), pp.59-65.

Schmelz, M., Schmidt, R., Ringkamp, M., Forster, C., Handwerker, H. and Torebjork, H. (1996). Limitation of sensitization to injured parts of receptive fields in human skin C-nociceptors. *Experimental Brain Research*, 109(1).

Story, G., Peier, A., Reeve, A., Eid, S., Mosbacher, J., Hricik, T., Earley, T., Hergarden, A., Andersson, D., Hwang, S., McIntyre, P., Jegla, T., Bevan, S. and Patapoutian, A. (2003). ANKTM1, a TRP-like Channel Expressed in Nociceptive Neurons, Is Activated by Cold Temperatures. *Cell*, 112(6), pp.819-829.

Stucky, C. and Lewin, G. (1999). Isolectin B(4)-positive and -negative nociceptors are functionally distinct. *Journal of Neuroscience*, 19(15), pp.6497-505.

Stutley, J., Cooke, J. and Parsons, C. (1989). Normal CT anatomy of the tongue, floor of mouth and oropharynx. *Clinical Radiology*, 40(3), pp.248-253.

Sugerman, P., Savage, N. and Young, W. (2000). Mucocele of the anterior lingual salivary glands (glands of Blandin and Nuhn): Report of 5 cases. *Oral Surgery, Oral Medicine, Oral Pathology, Oral Radiology, and Endodontology*, 90(4), pp.478-482.

Takeda, K., Kaisho, T. and Akira, S. (2003). TOLL-LIKE RECEPTORS. *Annual Review of Immunology*, 21(1), pp.335-376.

Takeuchi, O. and Akira, S. (2010). Pattern Recognition Receptors and Inflammation. *Cell*, 140(6), pp.805-820.

Trojanowski, J., Walkenstein, N. and Lee, V. (1986). Expression of Neurofilament Subunits in Neurons of the Central and Peripheral Nervous System: An Immunohistochemical Study with Monoclonal Antibodies. *The journal of Neuroscience*, 6(3), pp.650-660.

Trudler, D., Farfara, D. and Frenkel, D. (2010). Toll-Like Receptors Expression and Signaling in Glia Cells in Neuro-Amyloidogenic Diseases: Towards Future Therapeutic Application. *Mediators of Inflammation*, 2010, pp.1-12.

Wadachi, R. and Hargreaves, K. (2006). Trigeminal Nociceptors Express TLR-4 and CD14: a Mechanism for Pain due to Infection. *Journal of Dental Research*, 85(1), pp.49-53.

Wei, Y., Hu, S., Sun, B., Zhang, Q., Qiao, G., Wang, Z., Shao, R., Huang, G. and Qi, Z. (2017). Molecular cloning and expression analysis of toll-like receptor genes (TLR7, TLR8 and TLR9) of golden pompano (Trachinotus ovatus). *Fish & Shellfish Immunology*, 63, pp.270-276.

West, X., Malinin, N., Merkulova, A., Tischenko, M., Kerr, B., Borden, E., Podrez, E., Salomon, R. and Byzova, T. (2010). Oxidative stress induces angiogenesis by activating TLR2 with novel endogenous ligands. *Nature*, 467(7318), pp.972-976.

Woolf, C. and Ma, Q. (2007). Nociceptors—Noxious Stimulus Detectors. *Neuron*, 55(3), pp.353-364.

Yamamoto, T. (1975). Linguo-hypoglossal reflex: effects of mechanical, thermal and taste stimuli. *Brain Research*, 92(3), pp.499-504.

Zhao, H., Halicka, H., Traganos, F., Jorgensen, E. and Darzynkiewicz, Z. (2010). New biomarkers probing depth of cell senescence assessed by laser scanning cytometry. *Cytometry Part A*, 77A(11), pp.999-1007.

Zur, K., Mu, L. and Sanders, I. (2004). Distribution pattern of the human lingual nerve. *Clinical Anatomy*, 17(2), pp.88-92.